

Skeletal density of silica aerogels determined by helium pycnometry

A. AYRAL, J. PHALIPPOU, T. WOIGNIER

Laboratoire de Science des Matériaux Vitreux-U.A. 1119, Université de Montpellier II, 34095 Montpellier Cedex 05, France.

Density measurements of acid-catalysed aerogels have been carried out using helium pycnometry technique. The density increases from 1.85 to 2 when the volume percentage of tetramethoxysilane of the starting solution increases from 6 to 33. The aerogels submitted to an oxidation heat treatment show higher density values varying between 2 and 2.2. The variation of the skeletal density with the volume percentage of tetramethoxysilane is explained by a simple model taking into account the size of the primary particles which build the gel network. The observed difference between the measured density and the bulk density of amorphous silica (2.2) is attributed to the presence of organic residues located on the particles surface. The increase of skeletal density with the oxidation treatment is proposed to be due to the smoothing of the particle surface or to an increase of the particle size occurring during the oxidation treatment.

1. Introduction

Silica aerogels prepared from alcoholic solution of silicium alkoxides and submitted to supercritical drying of alcohol are materials which can easily be converted to fully dense silica glass.

Several studies have previously demonstrated that the solid part of aerogels prepared from silicon alkoxide possess a structure similar to vitreous silica [1, 2]. Aerogels have, however, high specific surface areas which result in particular properties. The aerogel surface is covered by different kinds of molecular species such as methoxy or hydroxyl groups. Infrared spectroscopy reveals the presence of both groups which means that methoxylation of the surface is not fully achieved during the supercritical drying step.

The skeletal density of gel can be considered a characteristic property of the material. The variation with temperature of the skeletal density can be used to appreciate the structural changes occurring during heat treatment. In the case of xerogels, it was previously demonstrated that skeletal density variations are linked to structural relaxation phenomena [3].

Density measurements are usually carried out using flotation or pycnometry techniques [4]. In the case of aerogels the microporosity, however, plays a very important role. It is very difficult to totally fill the pores even when the porosity is entirely open.

Helium pycnometry is expected to give the most reliable density values due to the very small size of the He atom, moreover, helium gas does not adsorb on silica surface at room temperature. This technique has been previously applied to silica aerogels. The results show that the skeletal density varies between 1.7 and 2.1 for the aerogels prepared [5, 6]. The density increases with the pH of the water used to carry out the

hydrolysis [6]. On the other hand, the skeletal density increases with the alkoxide content of the starting solution. Finally it was reported that oxidation heat treatments increase the skeletal density which reaches a value close to that of vitreous silica [6]. Recent works reported measurements carried out on oxidized aerogels [7]. Skeletal density values are in good agreement with our measurements.

In this study we investigate the variation of the skeletal density of aerogels prepared under acidic conditions as a function of the tetramethoxysilane content of the starting solution. Aerogels with the smallest skeletal density reputed were prepared. Models to explain this behaviour are proposed.

2. Experimental procedure

Silica alcogels are prepared by hydrolysis and polycondensation reactions of tetramethoxysilane (TMOS) diluted in methanol. The water used to perform the hydrolysis reaction is a 10^{-4} N HNO_3 solution. The volume fraction of TMOS (X) of the mixture varies between 6 and 33%.

The alcogels are then submitted to a methanol supercritical drying process. This treatment induces an esterification reaction which causes the aerogel to be hydrophobic by covering the surface of the aerogel with methoxy groups (OMe).

The surface methoxy groups can be removed with the help of a heat treatment carried out at 400°C for 5 h.

To avoid esterification reaction, a few alcogels are submitted to a supercritical drying treatment using liquid CO_2 . In this case, the initial solvent is gradually exchanged overnight with CO_2 .

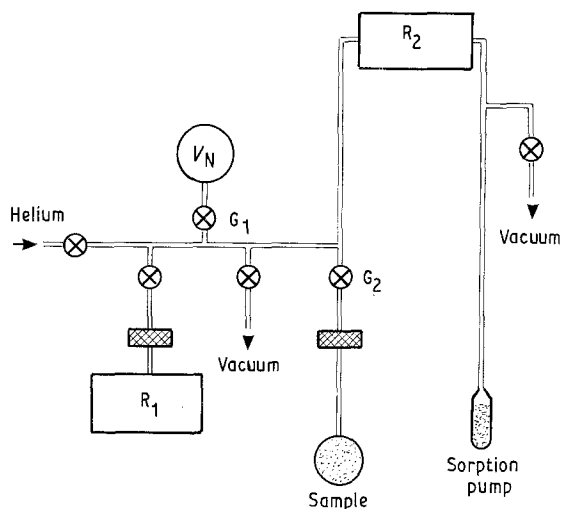


Figure 1 Schematic representation of apparatus allowing helium density measurements.

The sample volume is evaluated from pressure measurements using Mariotte's law. A vessel having a given volume, V_N , is first filled with helium gas at a pressure P_1 . Then the gas is allowed to fill the empty cell (without the sample) by opening valves G_1 and G_2 (Fig. 1). The pressure which establishes in the whole system is then P'_1 . The cell volume, V_T , is expressed by the following relation:

$$V_T = V_N \left(\frac{P_1}{P'_1} - 1 \right) \quad (1)$$

An identical measurement is performed with the cell filled with the aerogel powder (subscript 2).

In that case the volume of the sample, V_E , is given by the relation:

$$V_E = V_N \left(1 - \frac{P_2}{P'_2} \right) + V_T \quad (2)$$

The pressure values P and P' are given by a differential pressure sensor (R_2) which measures the pressure difference between the apparatus and another vessel maintained under vacuum by a sorption pump. The helium pressures range between 40 and 55 kPa. The measurement accuracy is about 1 Pa. The equipment is evacuated with a diffusion pump. A gauge (R_1) measures the vacuum in the cell. That gauge monitors the sample outgassing which is carried out at room temperature. More than 10 h are necessary to reach a vacuum level of 10^{-3} Pa (R_1). The weight of samples varies between 0.15 and 0.9 g depending on the aerogel apparent density. Samples are weighed after the volume measurement. The experiment is carried out in a thermostatically controlled room.

3. Results

The measured density of aerogels increases from 1.85 to 2 g cm^{-3} when X increases from 6 to 33% (Fig. 2). The scattering in density values of the different samples is not constant. Density measurements are more precise for samples having the highest apparent density. The average values are, however, much lower than for silica glass.

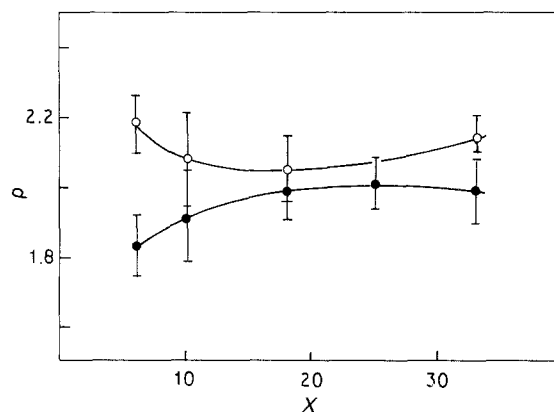


Figure 2 Skeletal density of silica aerogel as a function of TMOS content: full circles correspond to as prepared aerogels; open circles to oxidized aerogels.

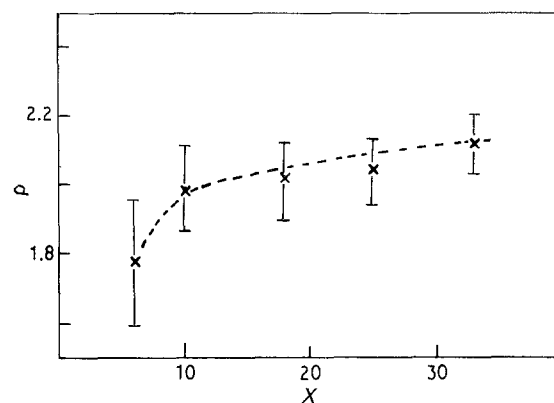


Figure 3 Skeletal density of CO_2 supercritical dried aerogels as a function of TMOS content.

The skeletal densities of aerogels are higher when the gels are submitted to an oxidation treatment. Skeletal density values close to the one of silica glass are then obtained. The skeletal density increases, however, when the silica content of the sol decreases.

Aerogels prepared by CO_2 supercritical drying exhibit a skeletal density which varies between 2 and 2.1 (Fig. 3). The lowest lightweight sample has a density lower than 2. Scattering in measurements is, however, important. It is noteworthy that the shape of the curve seems identical to that of classical methanol evacuated samples. The variation of the skeletal density with the TMOS content is identical to that observed for classical methanol evacuated samples.

4. Discussion

Even for a very small size molecule like He, a certain volume of the aerogel is not accessible. This volume is related to the smallest path approach, h_{He} , of the molecule to the material which was previously estimated to be about 0.05 nm [8]. The lost volume is related to the surface area of the material. Aerogels develop a specific surface area of several hundred $\text{m}^2 \text{ g}^{-1}$, thus this volume must be taken into account. On the other hand, we must consider that the texture

of aerogels is constituted by a wide distribution of pore sizes, some of them having diameters less than 2 nm. Helium molecules cannot fill the ultramicroporosity of the aerogels, moreover, the particle surface of aerogels is not smooth. This complex geometry has been previously described using the fractal concept [9]. Small angle neutron scattering (SANS) experiments show that the surface fractal dimension is close to 3 [10].

Another very important feature concerns the nature of the silica aerogel surface. Silica exhibits a strong tendency to undergo a hydroxylation reaction of its surface, which generally bears silanols (Si-OH) groups. The hydroxylation may be more or less complete. Fully hydroxylated silica surfaces have a density of 5 silanols per nm² [11].

Silanol groups linked to silica particles do not influence textural characteristic very much because of their low steric hindrance. This behaviour is clearly observed from the specific surface area of gels having different surface silanol contents [11].

Supercritical methanol drying is, however, performed at high temperature and high pressure. Under such conditions an esterification reaction of the gel surface occurs. Alcohol reacts with silanol groups and transforms them into alkoxy groups (Si-OR). The number of methoxy group per square nanometre can reach a value close to 5 [12, 13]. The area covered by one methoxy group is about 0.18 nm². Consequently the silica surface could be totally covered by methoxy groups if the esterification reaction is complete. Due to the presence of these lower density chemical species, the skeletal density of aerogel is less than that of dense silica.

In the following section the aerogel is assumed to be built up by an assembly of monodispersed spheres. The spheres are elementary units whose size varies between 1 and a few nanometres [14]. They are assumed to be made of pure dense silica. A sphere is connected to other neighbouring spheres by a single contact point. In other words we suppose that there is no interpenetration between spheres.

The mean coordination number n of a sphere may be estimated from the relation [15]

$$n = 2 \exp[2.4(1 - \phi)] \quad (3)$$

where ϕ is the porosity of the aerogel. For all the studied aerogels, ϕ is larger than 0.8. In this respect the porosity can be assumed to be totally open and fluids such as helium, methanol or water can freely flow within the pores (independently of kinetics that is related to solid permeability).

The specific surface area S_x measured using an adsorption method depends on several parameters linked to the nature of the adsorbing molecules and to the geometry of particles constituting the backbone of the material [11, 16].

$$S_x = \frac{3}{R\rho_{\text{SiO}_2}} \left(1 - \frac{nr_x}{4R^2} (2R + r_x) \right) \quad (4)$$

where R is the radius of the silica particle and r_x the radius of the adsorbing molecule.

Using relation 4 it is possible to evaluate the specific surface areas which would be measured using helium ($r_{\text{He}} = 0.05$ nm) or methanol ($r_{\text{Me}} = 0.18$ nm [17]) for different aerogel textures (Table I).

It is noteworthy that the formation of necks causes a decrease in the specific surface area. If the ratio a/R (where a is the radius of the neck) is close to 0.25 [16] the specific surface area decreases by about 5% as compared to the model of tangent spheres (last data of Table I).

Consequently the choice of the model of tangent spheres seems to be acceptable. Fig. 4 shows the porosity between spheres which is not filled by helium molecules. That phenomenon induces a decrease of measured skeletal density. The hatched region (Fig. 4) shows the half section g of that volume. The corresponding area is given by

$$g = \frac{1}{2} \left[R[(r_{\text{He}} + R)^2 - R^2]^{1/2} - r_{\text{He}} \sin^{-1} \left(\frac{R}{r_{\text{He}} + R} \right) - R \cos^{-1} \left(\frac{R}{r_{\text{He}} + R} \right) \right] \quad (5)$$

TABLE I Expected areas (m² g⁻¹) accessible for helium (He) and methanol (Me) molecules, for different size of primary particles having a mean coordination number n .

S_x	$R(\text{nm})$							
	0.5		1.0		1.5		5.0	
	He	Me	He	Me	He	Me	He	Me
$S_{n=0}$	2730	2730	1365	1365	910	910	270	270
$S_{n=2}$	2440	1570	1290	1100	880	795	270	265
$S_{n=3}$	2300	995	1260	960	865	735	270	260
$0.95S_{n=0}$	2595	2595	1300	1300	865	865	255	255

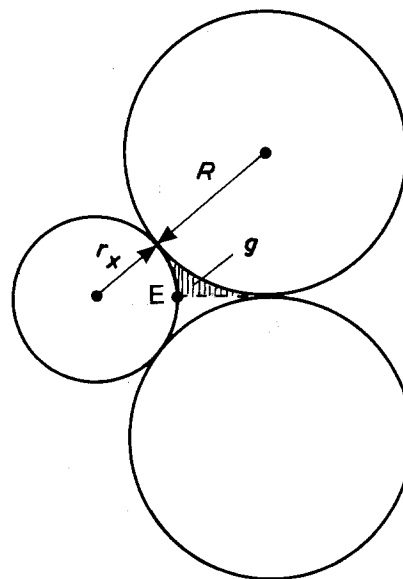


Figure 4 Schematic representation of the lost volume located between tangent particles.

The empty volume non-filled by helium molecule per sphere and per contact point is labelled f . It is approximately equal to g multiplied by the length of the ring corresponding to point E (Fig. 4)

$$f = g \{ R [(r_{\text{He}} + R)^2 - R^2]^{1/2} - r_{\text{He}} \} \quad (6)$$

Using these relations the skeletal density of aerogel can be estimated. The simplest calculation is first done for oxidized aerogels which exhibit only hydroxyl groups attached to their surface.

The considered mass of aerogel, m , corresponds to 1 g of silica and an additional mass related to the surface silanol. The silica network is composed by $[\text{SiO}_4]$ tetrahedra, each oxygen atom being shared between two tetrahedra. Concerning the surface silanols, only half the oxygen atom belongs to the silica network. Thus m is

$$m = 1 + \frac{5(M_{\text{H}} + 1/2M_{\text{O}}) \times 10^{18}}{N_{\text{A}}} S_{\text{He}} \quad (7)$$

where S_{He} is the specific surface area available for helium molecule (expressed in $\text{m}^2 \text{g}^{-1}$), M_{H} and M_{O} the atomic weights (expressed in atomic mass units; AMU) of the hydrogen and oxygen atoms, respectively, and N_{A} Avogadro's constant.

The calculation of the volume occupied by m g of aerogel, V , (expressed in cm^3) is more difficult to evaluate because of the additional "dead" volume which must be taken into account

$$V = \frac{1}{\rho_{\text{SiO}_2}} \left(1 + \frac{3n}{4\pi R^3 \times 10^{-24} f} \right) + 10^{-4} h_{\text{He}} S_{\text{He}} \quad (8)$$

$\begin{matrix} a & b_1 & b_2 & c \end{matrix}$

In that relation ($a \times b_1$) refers to the volume occupied by the pure silica, ($a \times b_2$) corresponds to the inaccessible volume located around the necks, and c is the usual lost volume when covering the surface with helium molecules [8]. The values of h_{He} and R are expressed in nm, the volume f in nm^3 and S_{He} in $\text{m}^2 \text{g}^{-1}$.

The skeletal density, ρ_0 , may be estimated from the ratio m/V for different n values. A minor change is observed (0.01 g cm^{-3}) when varying n from 2 to 3. The curve giving the mean value of ρ_0 as a function of R is shown in Fig. 5. SANS demonstrated that gyration radius increases with TMOS content of the starting solution. The evolution of the skeletal density with X is then expected to be identical to that observed with R .

The calculated skeletal densities are in good agreement with those measured. Differences are, however, observed for low R value (or X value). That difference is probably due to the fact that during oxidation treatment the neck radius must grow as a consequence of polycondensation reaction between silanols.

It is evident that the same calculation may be applied to CO_2 dried aerogels. In that case the skeletal density (Fig. 5) varies as predicted by the model.

The calculation of skeletal density of freshly dried gels is more complicated. In the above approach we have neglected the effect of surface silanol groups on

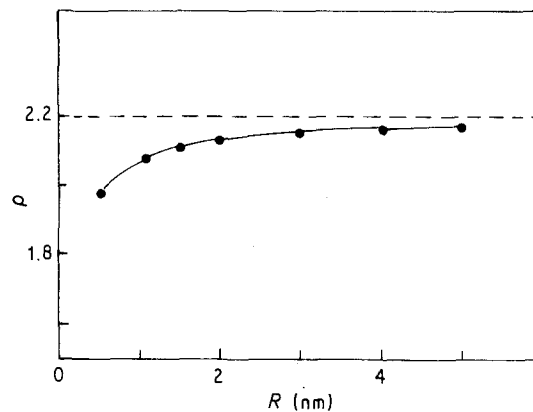


Figure 5 Variation of skeletal density with the radius of particles for an oxidized methanol-aerogel or a CO_2 aerogel.

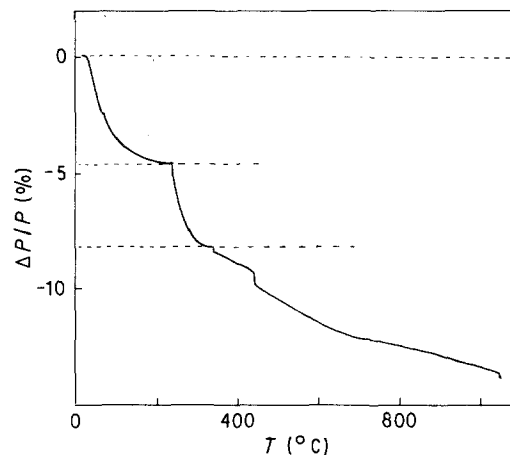


Figure 6 Weight loss versus temperature for an aerogel.

helium penetration. Without any oxidation treatment aerogels are covered by methoxy groups and such a simplification cannot be done. Thermogravimetric analyses have been performed to estimate the methoxy content of each aerogel. A typical curve for an aerogel $X = 25$ is given in Fig. 6. The weight loss recorded between room temperature and 200°C is attributed to the different chemical adsorbed species (H_2O , CH_3OH) which are weakly linked to the surface. The weight loss observed within the range 200 to 360°C is attributed to oxidation of methoxy groups [18].

It is assumed that no polycondensation reaction is occurring in this last temperature range. Dehydration of material is believed to start above 360°C . With this assumption the methoxy content corresponds to $1.5 \times 10^{-3} \text{ mol g}^{-1}$ of material.

The above estimated value is in good agreement with previously reported values [19]. With 5 groups per nm^2 the area covered by methoxy groups corresponds to $200 \text{ m}^2 \text{g}^{-1}$ of aerogel. In fact the specific surface attainable by methanol for such an aerogel is about $1000 \text{ m}^2 \text{g}^{-1}$. That means that only 1/4 (25%) of the surface is covered by methoxy groups. Given a methoxy group covers 0.18 nm^2 the thickness of the layer is estimated to be about 0.24 nm .

With this model the calculated density of freshly prepared aerogel, ρ_{F} , becomes

$$\rho_{\text{F}} = \frac{A}{B + C} \quad (9)$$

$$A = 1 + \frac{10^{18} [5 \times (M_{\text{CH}_3} + 1/2 M_0) \times 0.25 \times S_{\text{Me}} + 5(M_{\text{H}} + 1/2 M_0)(S_{\text{He}} - 0.25 S_{\text{Me}})]}{N_A} \quad (10)$$

where M_{CH_3} is the molecular mass of the CH_3 group (expressed in AMU).

$$B = \frac{1}{\rho_{\text{SiO}_2}} \left(1 + \frac{3n}{4\pi R^3 \times 10^{-24} f} \right)$$

$$C = 10^{-4} h_{\text{He}} \times 0.25 S_{\text{Me}} + 10^{-4} (h_{\text{Me}} + h_{\text{He}}) \times (S_{\text{He}} - 0.25 S_{\text{Me}})$$

The variation of ρ_F with R is plotted on Fig. 7 which corresponds to a n value of 2.5. Curves obtained for both $n = 2$ and $n = 3$ have the same shapes with a difference in ρ_F value decreasing when R increases. As an example the difference is 0.07 g cm^{-3} for $R = 0.5 \text{ nm}$ and 0.01 g cm^{-3} for $R = 1 \text{ nm}$.

SANS indicates that the particle size varies from 1.5 to 0.5 nm when X varies from 33 to 6%, respectively. The expected evolution of skeletal density with particle radius given by the model agrees well with experimental data.

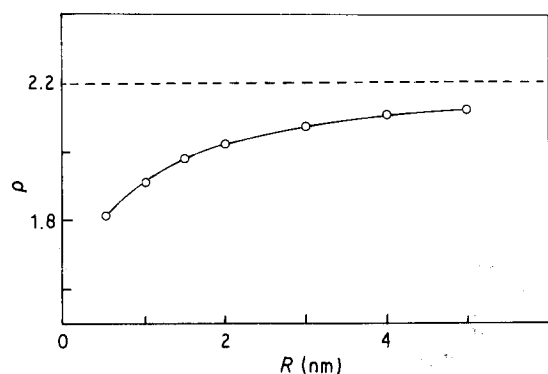


Figure 7 Variation of skeletal density with the radius of particles for an as prepared methanol-aerogel.

5. Conclusion

The small measured skeletal density values of aerogels prepared under acidic conditions is probably due to the small size of particles constituting the gel. The surface of aerogels is covered by a layer of methoxy groups which hinder helium penetration. The "solid" volume measured is thus much higher than the real one. Moreover, methoxy groups have a density lower than silica. As a consequence the measured density of the solid part of the aerogel is small compared to silica. A model including the two above mentioned

phenomena is proposed. It explains the evolution observed with the silica content of freshly prepared aerogels. When applied to oxidized samples it does not, however, account for higher skeletal densities of low silica content aerogels.

The discrepancy is believed to be due to neck size increase. Moreover, a surface smoothing appears as a consequence of the oxidation treatment that transforms methoxy groups into hydroxyl groups. A polycondensation reaction occurs between neighbouring silanol groups.

References

1. M. PRASSAS, J. PHALIPPOU and J. ZARZYCKI, *Glastech. Ber.*, **56K** (1983) 542.
2. G. E. WALRAFEN, M. S. HOKMABADI, N. C. HOLMES, W. J. NELLIS and SHENNING, *J. Chem. Phys.*, **82** (1985) 2472.
3. C. J. BRINKER, E. P. ROTH, G. W. SCHERER and D. R. TAILLANT, *J. Non-Cryst. Solids*, **71** (1985) 171.
4. N. TOHGE, G. S. MOORE and J. D. MACKENZIE, *ibid.* **63** (1984) 95.
5. F. J. BROEKER, W. HECKMANN, F. FISCHER, M. MIELKE, J. SCHROEDER and A. STANGE, in "Aerogels" edited by J. Fricke, (Springer, Berlin, 1986) p. 160.
6. T. WOIGNIER and J. PHALIPPOU, *J. Non-Cryst. Solids*, **93** (1987) 17.
7. A. H. BOONSTRA and C. A. M. MULDER, *ibid.* **105** (1988) 201.
8. S. LOWELL and J. E. SHIELDS, "Powder surface area and porosity" (Chapman and Hall, London, 1984).
9. D. W. SCHAEFER and K. D. KEEFER, *Phys. Rev. Lett.*, **53** (1984) 1383.
10. R. VACHER, T. WOIGNIER, J. PELOUS and E. COURTENS, *Phys. Rev. B*, **37** (1988) 6500.
11. R. K. ILER, "The chemistry of silica", (John Wiley, New York, 1979) pp. 485, 645.
12. B. C. BALLARD, E. C. BROGE, P. K. ILER, D. S. ST. JOHN and J. R. McWHORTER, *J. Phys. Chem.*, **65** (1961) 20.
13. T. ASANO and S. KITAHARA, *J. Chem. Soc. Japan, Pure Chem. Sect.*, **91** (1970) 109.
14. T. WOIGNIER, J. PHALIPPOU, R. VACHER, J. PELOUS and E. COURTENS, *J. Non-Cryst. Solids*, **121** (1990) 198.
15. H. P. MEISSNER, A. S. MICHAELS and R. KAISER, *Ind. Eng. Chem. Proc. Des. Div.*, **3** (1974) 202.
16. T. WOIGNIER and J. PHALIPPOU, *J. Non-Cryst. Solids*, **100** (1988) 404.
17. D. W. BRECK, "Zeolite molecular sieves, structure, chemistry and use", (John Wiley, New York, 1974) p. 633.
18. S. KONDO, H. FUJIWARA, E. OKAZAKI and T. ICHII, *J. Colloid Interf. Science*, **75** (1980) 328.
19. G. MAERTENS and J. J. FRIPIAT, *ibid.*, **42** (1973) 169.

Received 22 October 1990
and accepted 25 March 1991